ORIGINAL PAPER

Impact of arterial cross-clamping during vascular surgery on arterial stiffness measured by the augmentation index and fractal dimension of arterial pressure

M. T. Politi [1] · S. A. Wray [2,3] · J. M. Fernández [1] · J. Gaudric [4] · A. Ghigo [4] · P. Y. Lagrée [4] ·
C. Capurro [4] · J. M. Fullana [4] · R. Armentano [2,3]

Abstract Arterial cross-clamping is a common strategy used in vascular surgery and its duration is an independent predictor of surgical outcomes. The impact of arterial cross-clamping on the viscoelastic properties of the arterial system and its underlying mechanisms still remain unclear. The aim of this study was to evaluate the effect of arterial cross-clamping on arterial stiffness. A cross-sectional, observational, before-after study was designed to enroll adult patients undergoing vascular surgery. The Augmentation Index normalized to 75 beats-per-minute (AIx@75) and Fractal Dimension (FD) –indirect indicators of arterial stiffness– were calculated from radial arterial pressure tracings during surgery. The arterial pressure tracings from 8 patients were analyzed. Overall data included 4 aortic and 11 iliofemoral interventions. In both aortic and iliofemoral interventions, after arterial clamping, median AIx@75 rose and FD dropped significantly; the opposite occurred after arterial unclamping. Spearman's correlation suggests a strong significant negative correlation between median AIx@75 and FD during each hemodynamic state for aortic interventions. Our results are consistent at many levels: *a)* opposite events (i.e., clamping and unclamping) produce changes in different directions, *b)* two different indicators (i.e., AIx@75 and FD) suggest the same underlying phenomenon, and *c)* similar results are observed at different vascular locations (i.e., aortic and iliofemoral). Overall, our data consistently suggests an increase in arterial stiffness during clamping and a reduction during unclamping. Despite the large distance from the aortic or iliofemoral intervention sites, radial artery pressure monitoring is still able to detect consistently these vascular events.

Keywords Augmentation index · Fractal dimension · Arterial pressure · Vascular surgery · Cross-clamping

This article is part of the Topical Collection on *Health and Technology in Latin America*

M. T. Politi and S. A. Wray contributed equally to this work.

✉ M. T. Politi
teresapoliti@yahoo.com.ar

1 Laboratorio de Biomembranas. Instituto de Fisiología y Biofísica Bernardo Houssay (IFIBIO Houssay). CONICET-UBA, Departamento de Ciencia Fisiológicas, Facultad de Medicina, Universidad de Buenos Aires, Paraguay 2155, C1121ABG Buenos Aires, Argentina

2 Escuela de Estudios Avanzados en Ciencias de la Ingeniería, Universidad Tecnológica Nacional (EEACI - UTN), Sarmiento 440, C1041AAJ Buenos Aires, Argentina

3 Universidad Favaloro, Solís 453, C1078AAI Buenos Aires, Argentina

4 Institut Jean Le Rond d'Alembert, Sorbonne Universités, UPMC, Paris 06, CNRS, UMR 7190, F-75005 Paris, France

1 Introduction

Arterial cross-clamping is a necessary strategy for vascular surgery procedures, such as aortic aneurysm repair or peripheral vascular bypass [1]. Within the human vascular network, the aorta is the most thoroughly studied vessel during cross-clamping procedures [2]. Both arterial clamping and unclamping can produce several clinical disturbances, such as myocardial infarction, heart failure, acute lung injury, co-agulopathies, visceral ischemia, acute kidney failure, and eventually, postoperative multiorgan failure and death [3–7]. In clinical studies, the clamping time of aortic cross-clamping has shown to be an independent predictor of overall surgical outcomes [8]. Some of the proposed pathophysiological mechanisms behind these clinical outcomes are ischemia and reperfusion injury, oxidative stress damage, systemic

inflammatory response, and microcirculatory dysfunction [9–13]. However, the impact of arterial cross-clamping on the viscoelastic properties of the arterial system and its underlying mechanisms remain unclear. Furthermore, the comparative effects of clamping and unclamping common vascular surgery sites (such as the aorta and the iliofemoral artery) on the biomechanical characteristics of the vascular system have not been systematically studied.

We hypothesized that arterial clamping and unclamping would produce significant changes in the viscoelastic properties of the vascular system, mainly affecting arterial stiffness. A practical approach towards studying arterial stiffness is to analyze the morphology of the arterial pressure wave under different hemodynamic states. The Augmentation Index (AIx) and the Fractal Dimension (FD) of arterial pressure are indexes that are commonly used as indirect measures of wave reflections and arterial stiffness [14]. One of the main advantages of these vascular indexes is that they can be assessed with pressure wave morphology only [15].

The augmentation index (AIx) is a ratio calculated from the analysis of blood pressure waveform morphology. It is defined as the augmentation pressure (i.e., the difference between the late systolic pressure shoulder and the early systolic pressure shoulder) divided by the pulse pressure (i.e., the difference between the maximum systolic pressure and the end diastolic pressure), and is usually expressed as a percentage (Fig. 1) [16]. The AIx is a measure of the relative contribution of wave reflection to the systolic arterial pressure [17]. Under normal conditions, the arterial pressure waveform is determined by the sum of a forward traveling wave coming from the heart, and backward reflected waves coming from the periphery

vessels. The amplitude and propagation speed of the reflected waves depend on the peripheral resistance and on the functional and structural characteristics of the arterial network [18–20]. For example, arterial stiffening increases the speed of propagation of both forward and backward waves, resulting in an earlier return of reflected waves, a higher degree of overlap among forward and backward waves, and a change in the morphology and amplitude of the waveform [21–23]. Therefore, both the magnitude and the sign of the AIx provide information on arterial pressure wave morphology and, indirectly, on arterial stiffness and the influence of wave reflections [24].

Arterial pressure waves can be classified into three different wave types according to wave morphology, which can be quantified through their AIx value (Fig. 1) [25]. A study of the aortic input impedance (i.e., a measure of effective hemodynamic resistance) in human subjects undergoing catheterism, proposed that the variations in pressure waveforms are due to differences in wave reflections in the arterial tree. Type A waves suggest considerable reflection in the arterial system, while type C waves imply smaller or more diffuse reflections. Type B waves would be an intermediate pattern between the two [26].

The Fractal Dimension (FD) of arterial pressure in another indirect index for arterial stiffness. A fractal is a set of data that shows self-similarity throughout a certain dimension (e.g. time or space), which means it has a repeating pattern at every scale. The vascular system may have a fractal architecture related to its open tree structure, which is based on repeated bifurcations [27]. The fractal character of the vascular system is produced by *a)* the fact that the same general rule or pattern of dichotomous divisions is applied in the growth of each portion of the tree from the previous
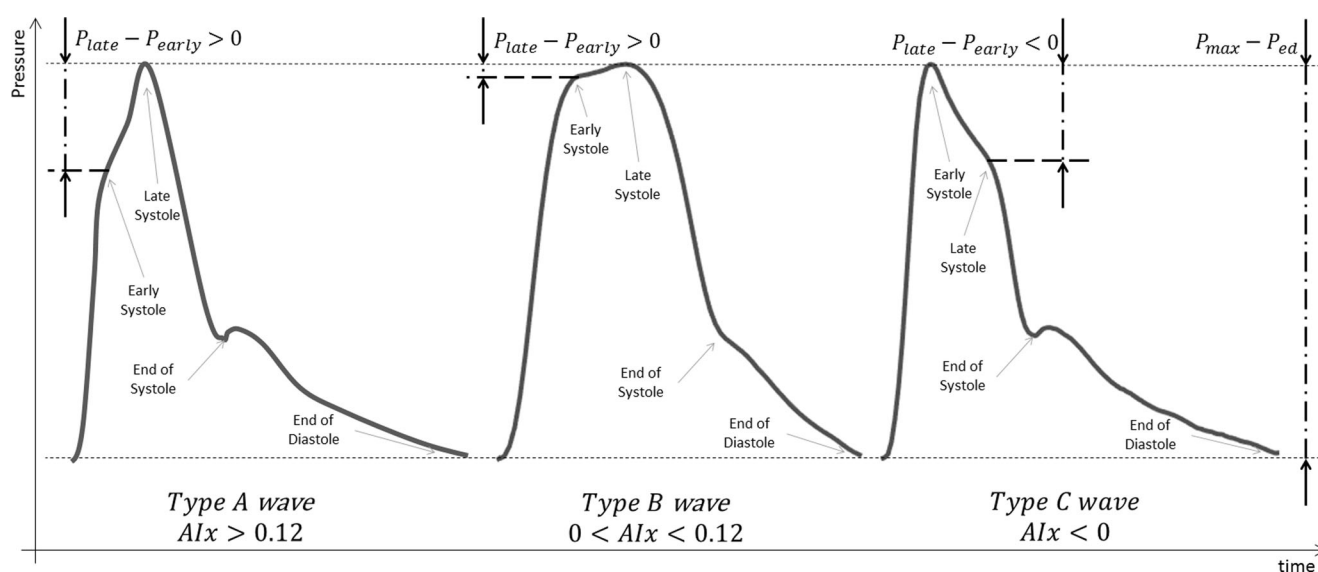
Fig. 1 Classification of arterial pressure waves according to wave morphology. In type A waves the early systolic pressure shoulder is lower than the late systolic pressure shoulder and the Augmentation Index (AIx) has a positive value, which is above 0.12. Type B waves are similar to type A waves except for the fact that the AIx has a positive value below 0.12. In type C waves the early systolic pressure shoulder is higher than the late systolic pressure shoulder and the AIx has a negative value

portion, and *b)* a self-similarity shown at many different levels; for example, in the fact that any portion the tree, taken as a whole, has the same branching structure as the overall tree [28]. Similarly, flow distributions in the systemic circulation may also follow a fractal pattern since its arrangement is heterogeneous, although not random. A fractal characterization of blood flow may arise from the logarithmic relation between flow dispersion and element size, showing an increase in the degree of heterogeneity as the size of the elements decrease. The fractality of blood flow could be related to the fact that flow is delivered through a branching vascular tree, which appears to have a fractal structure itself [29]. Arterial blood pressure may also have an underlying fractal structure that could describe the multiple changes in the waveform complexity of arterial pressure time series [30, 31].

Daily physiological variations and adjustments of the cardiovascular system have a complex behavior that is related to the inherent complexity of its own structure [32]. A straightforward way of measuring this complex behavior is by determining the FD of a given time-based parameter of the cardiovascular system. Conceptually, the FD is a way of quantifying the self-similarity of a parameter (e.g. blood pressure) throughout a dimension (e.g. time), that is, a measure of resemblance at different observation scales [33]. Fractal physiological signals –such as blood pressure– may lose their fractal nature (i.e., decrease their FD) in pathological states, thus making FD an indicator of cardiovascular health. Previous in-vitro studies show that the loss of fractal complexity of blood pressure is related to an increase in arterial stiffness. [31] Clinical studies have also suggested that FD may be have diagnostic and prognostic value in patients with heart failure and could be a predictor of mortality [32].

The aim of this study is to evaluate the impact of arterial cross-clamping on the biomechanical properties of the vascular system by using data from continuous radial arterial pressure tracings during vascular surgery. We chose AIx and FD as indirect indicators of the arterial stiffness of the vascular network for several hemodynamic states. We proposed that the clamping and unclamping events during vascular surgery would have a significant impact on these indicators. We additionally sought to explore the relationship between these two indicators throughout the vascular surgery.

2 Methods

2.1 Study design

A cross-section, observational, analytical, before-after study was designed. We evaluated the effect of arterial clamping and unclamping during vascular surgery at two different locations in the vascular network: iliofemoral and infrarenal abdominal aorta. The effect of these interventions on arterial stiffness was estimated indirectly by the Augmentation Index normalized to 75 beats-per-minute (AIx@75) and the Fractal Dimension (FD) of invasive radial arterial pressure tracings during each clamping condition.

2.2 Patient enrolment

The study enrolled adult patients undergoing peripheral vascular surgery at the *Hôpital Universitaire Pitié-Salpêtrière* in Paris, France. Exclusion criteria were having *a)* an irregular heart rhythm, or *b)* an undetectable pressure notch. The study protocol was approved by the IRB of the *Hôpitaux Universitaires La Pitié-Salpêtrière*. The study is in accordance with the ethical principles of the Declaration of Helsinki [34].

2.3 Invasive radial arterial pressure measurements

Experimental data were obtained from continuous invasive arterial pressure measurements using a fluid-filled catheter from the radial artery of adult patients undergoing peripheral vascular surgery. We used a disposable pressure transducer (TruWave, Edwards Lifesciences®) with a natural frequency of 40 Hz for a standard kit for measuring blood pressure. Data were registered using an analogue-digital converter with internal hardware filters ((low pass frequency set at 20 kHz, high pass frequency set at 0.05 Hz, MP150, BIOPAC Systems Inc.) and the AcqKnowledge software. Data acquisition rate was 100 Hz.

2.4 Waveform analysis

A stable set of beats from radial arterial pressure tracings were chosen manually throughout a 20-s interval immediately before and after each clamp and unclamp event. A brief transitional period was allowed after each event. The time values for end diastolic, end systolic, early systolic shoulder, late systolic shoulder and maximum pressure were computed for each beat with a custom software developed in Matlab (R2014b, The MathWorks, Inc., Natick, Massachusetts). The median heart rate (HR) was calculated using the foot-to-foot time differences of the radial arterial pressure.

In order to identify the early and late systolic pressure shoulders, a two-term Gaussian model was used to separate the first and second components of the systolic portion of each beat, where the modeled systolic pressure ($P_S(t)$) for each beat was expressed as [35]:

$$P_S(t) = a_1 \cdot e^{-\left(\frac{t-b_1}{c_1}\right)^2} + a_2 \cdot e^{-\left(\frac{t-b_2}{c_2}\right)^2}$$

This method has shown to yield good results when modeling peripheral pressure waveforms [35, 36] In our data, we

estimated for each beat the coefficient of determination (R^2) between the model and the data. The minimum value for all beats from all patients in all states was $R^2 = 0.987$.

The time centroids b_1 and b_2 were recorded and their difference was established as the time-distance between the early and late systolic pressure shoulders. The maximum pressure was assigned to one of the shoulders, depending on the wave morphology (i.e., type A, type B or type C) (Fig. 1) [26]. The other shoulder was located by using the time difference between centroids (e.g., in a type C beat, the maximum pressure matches the early shoulder, while the late shoulder is found $|b_2 - b_1|$ seconds later). This technique produced successful results that were visually validated, and double-checked using the method described by Takazawa et al. [14, 37].

The Augmentation Index (AIx) was calculated as following:

$$AIx = \frac{P_{late} - P_{early}}{P_{max} - P_{ed}} \cdot 100$$

where P_{late}, P_{early}, P_{max} and P_{ed}, are late systolic pressure, early systolic pressure, maximum systolic pressure, and end diastolic pressure, respectively. All AIx values were normalized to a heart rate of 75 beats-per-minute (AIx@75), using the well-known conversion formula [38]:

$$AIx@75 = AIx - 0.39 \cdot (75 - HR)$$

The Fractal Dimension (FD) was calculated for each set of data using a custom software developed in Matlab following the Higuchi method [39]. The software was validated using several fractal signals with a known FD, yielding acceptable mean and SD values (test signal: FD = 1.2; calculated FD = 1.231 ± 0.069; test signal: FD = 1.5; calculated FD = 1.514 ± 0.134).

The Higuchi method uses different scales to measure the length of the curve of a given parameter [39]. The log-log relationship between the resulting lengths and their corresponding scales is given by:

$$L(k) \propto k^{-FD}$$

where $L(k)$ is the measured length with the scale k.

As in most natural phenomena, FD may not be constant over all time scales. Instead, there are two ranges in which the property of self-similarity holds, which are separated by a critical breaking point [39]. FD was calculated for all scales, and the critical point where lower and higher ranges break was detected by optimizing the linear adjustments of the length L(k). The reported FD value is the median FD for the lower range scales.

2.5 Statistical analysis

Since FD and AIx@75 distributions deviate from normal when tested formally (AIX@75 has a skewed distribution and FD has a logarithmic distribution), data are presented as median and interquartile range (IQR) and non-parametric tests were chosen. The statistical analysis involved Wilcoxon matched-pairs signed-ranks test for before-after testing and Spearman's rank-order correlation using R studio free statistical software. All statistical tests were two-tailed. Statistical significance was considered at 5 % ($\alpha = 0.05$).

3 Results

3.1 Patient clinical data

The radial arterial pressure tracings of 9 patients undergoing vascular surgery were evaluated in this study; one patient was excluded for having an irregular heart rhythm. The arterial pressure tracings from a total final of 8 patients were analyzed. The surgeries involved were 4 infrarenal abdominal aorta prosthesis placements and 4 iliofemoral bypass surgeries. Some surgeries required more than one arterial intervention; overall, there were 4 aortic and 11 iliofemoral interventions. Mean age was 69 years. Most patients were non-diabetic males with hypertension who were current or former smokers. All patients had a baseline type C waveform. Of the 60 hemodynamic states analyzed, 58 hemodynamic states had type C waveforms; only one patient switched to a type A waveform during two hemodynamic states. Table 1 displays main patient clinical characteristics. Figure 2 illustrates the results of one representative patient.

Table 1 Patient clinical characteristics

	($n = 8$)
Age - years	68.9 ± 14.5
Males - no (%)	5 (62.5)
Hypertension	6 (75.0)
Hypercholesterolemia	7 (87.5)
Diabetes	0 (0.0)
Smokers	5 (62.5)
Pack-year among smokers	46.3 ± 24.3
BMI – kg/m^2	23.8 ± 3.3
Baseline type C waveform –no (%)	8 (100.0)

Data are presented as mean ± SD. *BMI* body mass index
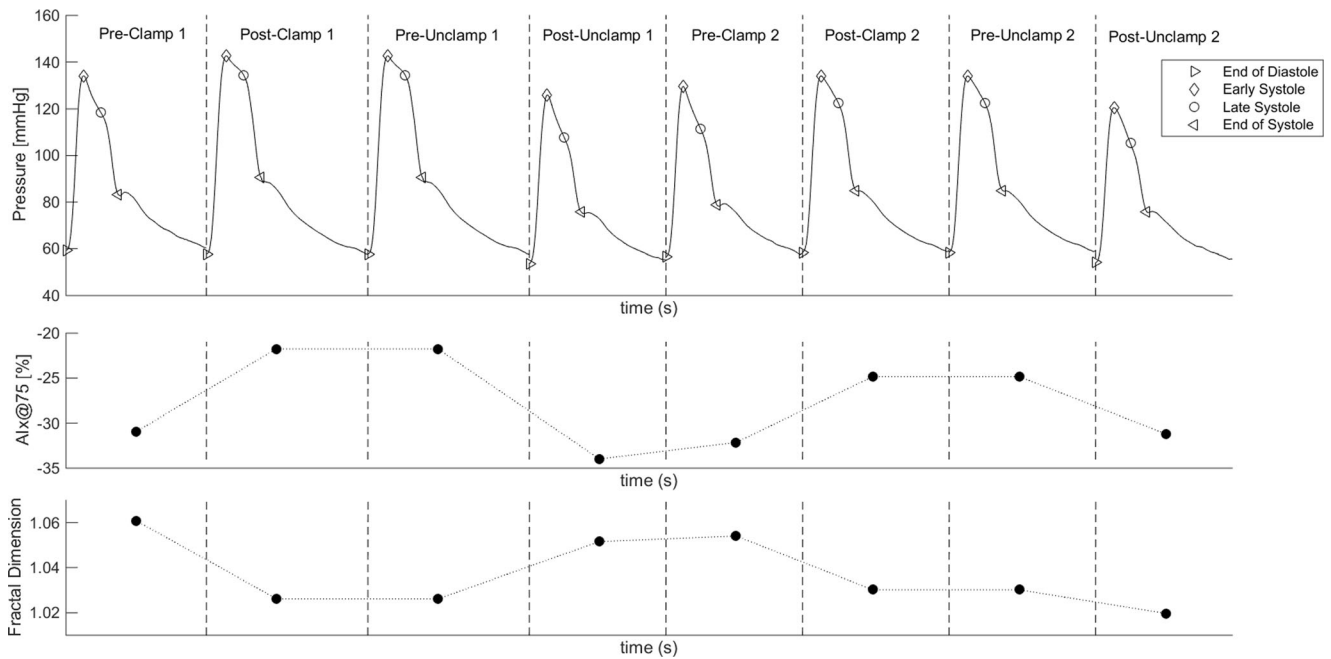
Fig. 2 Average arterial radial pressure tracings over 20-s intervals before and after each event (clamping/unclamping) for one representative patient undergoing vascular surgery. The end of diastole, end of systole, early systole and late systole pressures were detected on arterial pressure tracings. The Augmentation Index normalized to 75 beats-per-minute (AIx@75) and the Fractal Dimension (FD) were calculated for each state

3.2 Augmentation index normalized to 75 beats-per-minute (AIx@75)

Experimental data included continuous invasive radial arterial pressure tracings from 4 infrarenal abdominal aorta clamps and unclamps, and from 11 iliofemoral artery clamps and unclamps.

Table 2 presents the overall results for the median AIx@75 over a 20-s interval before and after aortic clamping and unclamping for all aortic interventions. After infrarenal abdominal aorta clamping, the median AIx@75 increased significantly (−14.8 to −14.2; ΔAIx@75 + 4.1 %; $p < 0.01$), while after unclamping, it decreased significantly (−0.142 to −0.177; ΔAIx@75–24.6 %; $p < 0.001$). Notice that the sign of the median AIx@75 remained unchanged after both clamping and unclamping events.

Table 3 presents the overall results for the median AIx@75 over a 20-s interval before and after iliofemoral artery clamping and unclamping for all iliofemoral interventions. After iliofemoral artery clamping, the median AIx@75 increased significantly (−15.9 to −13.9; ΔAIx@75 + 12.6 %; $p < 0.001$), while after unclamping, it decreased significantly (−15.3 to −15.7; ΔAIx@75–2.6 %; $p < 0.001$). Once again, the sign of the median AIx@75 remained unchanged after both clamping and unclamping events.

3.3 Fractal dimension (FD)

Table 4 shows data for the median FD over a 20-s interval before and after aortic clamping and unclamping for all aortic interventions. After infrarenal abdominal aorta clamping, the median FD was reduced significantly (1.039 to 1.027; ΔFD −1.2 %; $p < 0.01$), while after unclamping, it increased significantly (1.031 to 1.040; ΔFD + 0.9 %; $p < 0.001$).

Table 5 shows data for the median FD over a 20-s interval before and after iliofemoral artery clamping and unclamping for all iliofemoral interventions. After iliofemoral artery clamping,

Table 2 Changes in Augmentation Index normalized to 75 beats-per-minute (AIx75) following **aortic** clamp and unclamp

Pre-clamp		Post-clamp			
Median	IQR	Median	IQR	ΔAIx@75 (%)	p
−14.8	−20.7 to −2.9	−14.2	−20.6 to −10.6	+4.1	<0.01
Pre-unclamp		Post-unclamp			
Median	IQR	Median	IQR	ΔAIx@75 (%)	p
−14.2	−20.9 to 10.0	−17.7	−34.1 to −07.4	−24.6	<0.001

IQR interquartile range. ΔAIx@75 (%): relative percentage change in AIx

Table 3 Changes in Augmentation Index normalized to 75 beats-per-minute (AIx75) following **iliofemoral** clamp and unclamp

Pre-clamp		Post-clamp			
Median	IQR	Median	IQR	ΔAIx@75 (%)	p
−15.9	−19.8 to −11.0	−13.9	−17.3 to −05.5	+12.6	<0.001
Pre-unclamp		Post-unclamp			
Median	IQR	Median	IQR	ΔAIx@75 (%)	p
−15.3	−17.5 to −8.8	−15.7	−19.0 to −10.8	−2.6	<0.001

IQR interquartile range. ΔAIx@75 (%):relative percentage change in AIx

the median FD was reduced significantly (1.032 to 1.029; ΔFD −0.3 %; $p < 0.01$), while after unclamping, it increased significantly (1.029 to 1.033; ΔFD + 0.4 %; $p < 0.001$).

3.4 Correlation between augmentation index normalized to 75 beats-per-minute (AIx@75) and fractal dimension (FD)

In the light of these results, we decided to explore the relationship between the two indicators, median AIx@75 and FD, during different hemodynamic states through Spearman's rank-order correlation. The relation between these variables was monotonic, though non-linear, as assessed by visual inspection of a scatterplot. A strong significant negative correlation between median AIx@75 and FD for each hemodynamic state was found for aortic interventions (($r_s = -0.95$; $p < 0.05$), though not for iliofemoral interventions nor overall data. These results are illustrated in Fig. 3.

4 Discussion

The results show that arterial clamping and unclamping during vascular surgery have a significant impact on the biomechanical properties of the vascular system, as assessed by the Augmentation Index normalized to 75 beats-per-minute (AIx@75) and the Fractal Dimension (FD), calculated from radial arterial pressure tracings. After arterial clamping, median AIx@75 rises and median FD drops; the opposite occurs after arterial unclamping. This effect was observed in both aortic and iliofemoral interventions.

The increase in the median values of AIx@75 during arterial clamping may indicate a higher arterial stiffness during this hemodynamic state [14, 40]. However, the magnitude of this effect on median AIx@75 was relatively small (4.1 % in aortic interventions and 12.6 % in iliofemoral interventions). Additionally, the sign of the median AIx@75 did not change, which possibly indicates that the increase in arterial stiffness was not large enough to change the wave morphology into a type A or B wave. The decrease in median FD during arterial clamping also suggests a higher arterial stiffness [31, 33]. Once again, the magnitude of this effect on median FD was small (1.2 % in aortic interventions and 0.3 % in iliofemoral interventions). Despite the small effect size, our results are consistent at many levels: *a)* opposite events (i.e., clamping and unclamping) produce changes in different directions, *b)* two different indicators (i.e., AIx@75 and FD) suggest the same underlying phenomenon, and *c)* similar results are observed at different vascular locations (i.e., aortic and iliofemoral). Overall, our data consistently suggests an increase in arterial stiffness during clamping and a reduction in arterial stiffness during unclamping.

Similar results were published by Armentano et al. by measuring the simultaneous aortic pressure and diameter in 14 conscious dogs before and after occluding the distal descending aorta with a pneumatic cuff [14]. These authors observed that, during aortic occlusion, the aortic pressure FD decreased and the pressure-strain elastic modulus (E) of the aortic wall increased (i.e., the aorta became stiffer). The magnitude of the FD drop reported by these authors was −4.7 %, which is only slightly higher than our own findings, −1.2 % (1.039 to 1.027; $p < 0.01$), especially when taking into account that *a)* our

Table 4 Changes in Fractal Dimension (FD) following **aortic** clamp and unclamp

Pre-clamp		Post-clamp			
Median	IQR	Median	IQR	ΔFD (%)	p
1.039	1.006 to 1.154	1.027	1.004 to 1.135	−1.2	<0.01
Pre-unclamp		Post-unclamp			
Median	IQR	Median	IQR	ΔFD (%)	p
1.031	1.004 to 1.138	1.040	1.007 to 1.178	+0.9	<0.001

IQR interquartile range. ΔAIx@75 (%):relative percentage change in AIx

Table 5 Changes in Fractal Dimension (FD) following **iliofemoral** clamp and unclamp

Pre-clamp		Post-clamp			
Median	IQR	Median	IQR	ΔFD (%)	P
1.032	1.005 to 1.154	1.029	1.003 to 1.138	−0.3	<0.01
Pre-unclamp		Post-unclamp			
Median	IQR	Median	IQR	ΔFD (%)	p
1.029	1.004 to 1.143	1.033	1.005 to 1.151	+0.4	<0.001

IQR interquartile range. ΔAIx@75 (%): relative percentage change in AIx
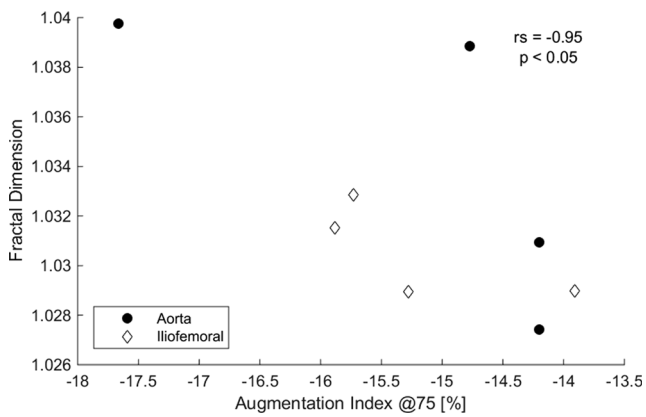
Fig. 3 Spearman's rank-order correlation between the Augmentation Index normalized to 75 beats-per-minute (AIx@75) and the Fractal Dimension (FD). A strong significant correlation between median AIx@75 and FD for each hemodynamic state was found for aortic interventions ($r_s = -0.95$; $p < 0.05$), though not for iliofemoral interventions nor overall data

protocol involved a more distal occlusion site (infrarenal aorta instead of descending aorta), and *b)* our protocol involved a larger distance between the pressure measurement site (i.e., radial artery) and the occlusion site (i.e., infrarenal aorta or iliofemoral artery) whereas Armentano et al. measured the aortic pressure just proximal to the occlusion site. Therefore, these results would be in accordance with our own findings.

Given this apparent association between changes in arterial stiffness and changes in AIx@75 and FD, what remains to be addressed are the possible underlying mechanisms involved. Armentano et al. suggest that reflected waves may participate in changes in FD during arterial occlusion. Through wave separation analysis, these authors studied the forward and backward traveling components of the aortic pressure wave before and after the occlusion of the descending aorta in dogs. The authors analyzed only the first two heartbeats after aortic occlusion, as to avoid the participation of regulation mechanisms (which take place around the fifth heartbeat after occlusion) in the resulting waveform. They proposed that, during total occlusion of the descending aorta, aortic incident waves reflect almost completely and immediately at the descending aorta occlusion site, thus overlapping the incident wave with the reflected wave and increasing overall aortic pressure and modifying waveform morphology. Since multiple branching reflection sites are avoided during aortic occlusion, the fractal complexity of the aortic pressure wave is reduced (i.e., aortic FD decreases). The authors conclude that arterial pressure fractality depends highly on the wave reflection [14]. In the light of these conclusions, in our results, the decrease in median FD during clamping could be associated to loss in the complexity of the pressure waveform due to reduced reflection sites during clamping. Additionally -and since in our own protocol both AIx@75 and FD were calculated from 20-s intervals before and after each event- reflex regulation

mechanisms (i.e., reduced heart rate and increased contractile force) probably pay a contribution to the waveform structure in our analysis, as in actual real-life patients.

Murgo et al. also studied the aortic pressure waveform after arterial occlusion [26]. These authors invasively measured pressure in the ascending aorta of 4 patients undergoing coronary catheterism after the external occlusion of the iliac artery. These authors describe significant changes in the aortic waveform related to an increase in the late systolic pressure shoulder, without observing changes in the end-diastolic pressure. Just as in our protocol, the authors measure the arterial pressure at a distant site from the vascular occlusion; however, it is still a *central* arterial pressure measurement. Therefore, the effect of reflection waves may be larger than on *peripheral* arterial pressure measurements [41]. Through the study of the impedance spectral patterns, these authors suggest that type A waveforms are associated to a stiffer vascular profile, with considerable wave reflections returning from the periphery; whereas type C waves imply smaller or more diffuse reflections [26]. Our results are in accordance with these reports, since clamping increased the magnitude of AIx@75, although the waveform type did not change.

Cymberknop et al. studied the variation of the complexity of the arterial pressure waveform in relation to its anatomical location. The authors compared the continuous arterial pressure waveforms of the carotid and femoral arteries through non-invasive applanation tonometry in human subjects. They found that the arterial pressure FD of the carotid artery was higher than the arterial pressure FD of the femoral artery ($+56.51 \pm 13.62$ %). Though the authors did not evaluate clamping or unclamping interventions, these findings could possibly indicate that the higher pressure FD reported in the carotid artery is related to a higher waveform complexity, due to a higher exposure to multiple wave reflection at central vascular sites. The lower pressure FD reported in the femoral artery could be related to the loss of complexity at vascular sites distant from the heart pump, a process often described as an 'unwrinkling' phenomenon [30]. This 'unwrinkling' phenomenon or loss of complexity could also possibly occur during arterial clamping, and would explain the decrease in pressure FD during clamping and its increase during unclamping.

Finally, although wave reflections occur at multiple locations in the arterial system, in human subjects the "effective" reflection site is the region of the terminal abdominal aorta and the bifurcation of the iliac and femoral arteries [26, 42, 43]. These vessels would produce reflections that dominate over those arising from other locations. The fact that the surgical interventions of our study are located at the dominant reflection sites suggests that reflection waves could participate in the observed changes in AIx@75 and FD.

As opposed to others, our results have demonstrated changes in arterial pressure AIx@75 and FD during clamping with an effect size smaller than previously reported [14, 26].

However, these studies involved intraortic measurements in invasive animal experiments or in human subjects undergoing coronary catheterization. Our study analyzed the arterial pressure AIx@75 and FD through a radial artery catheter, which is a minimally-invasive monitoring instrument that is widely-used in surgical settings. Despite the large distance from the event taking place at the aortic or iliofemoral intervention sites, radial artery pressure monitoring was still able to detect consistently these vascular events.

The question on the role of FD in hemodynamic monitoring and in the study of the viscoelastic properties of the vascular network is yet to be answered. Due to the influence of peripheral reflected waves on this index, the FD may be able to address issues related to peripheral microcirculation, such as the skin or retinal vessels [44–46]. As a measure of complexity, it may also have a higher capacity than the AIx to discriminate the incident wave and the reflected wave in the overall waveform.

In summary, in both the aorta and the iliofemoral artery, arterial clamping and unclamping significantly modify the Augmentation Index normalized to 75 beats-per-minute (AIx@75) and the Fractal Dimension (FD) measured by invasive radial arterial pressure monitoring, suggesting changes in arterial stiffness. After arterial clamping, median AIx@75 rises and median FD drops; the opposite occurs after arterial unclamping. A strong significant negative correlation between median AIx@75 and FD for each hemodynamic state was found for aortic interventions ($r_s = -0.95$; $p < 0.05$), though not for iliofemoral interventions nor overall data. Overall, our data consistently suggests an increase in arterial stiffness during clamping and a reduction during unclamping.

Compliance with ethical standards

Conflict of interest The authors declare that they have no conflict of interest.

References

1. Dalman R. Operative techniques in vascular surgery. Lippincott Williams & Wilkins; 2015.
2. Gelman S. The pathophysiology of aortic cross-clamping and unclamping. J Am Soc Anesthesiol. 1995;82(4):1026–57.
3. Katseni K, Chalkias A, Kotsis T, Dafnios N, Arapoglou V, Kaparos G, Logothetis E, Iacovidou N, Karvouni E, Katsenis K. The Effect of Perioperative Ischemia and Reperfusion on Multiorgan Dysfunction following Abdominal Aortic Aneurysm Repair. BioMed Res Int, 2015.
4. Lim S, Halandras PM, Saqib NU, Ching YA, Villella E, Park T, Son H, Cho JS. Comparison of supramesenteric aortic cross-clamping with supraceliac aortic cross-clamping for aortic reconstruction. J Vasc Surg, 2016.
5. Wartman SM, Woo K, Yaeger A, Sigman M, Huang SG, Ham SW, et al. Outcomes after abdominal aortic aneurysm repair requiring a suprarenal cross-clamp. J Vasc Surg. 2014;60(4):893–9.
6. Wynn MM, Acher C, Marks E, Engelbert T, Acher CW. Postoperative renal failure in thoracoabdominal aortic aneurysm repair with simple cross-clamp technique and 4 C renal perfusion. J Vasc Surg. 2015;61(3):611–22.
7. Kotake Y, Yamada T, Nagata H, Takeda J, Shimizu H. Descending aortic blood flow during aortic cross-clamp indicates postoperative splanchnic perfusion and gastrointestinal function in patients undergoing aortic reconstruction. Br J Anaesth 2012;aes095.
8. Svensson LG, Crawford ES, Hess KR, Coselli JS, Safi HJ. Experience with 1509 patients undergoing thoracoabdominal aortic operations. J Vasc Surg. 1993;17(2):357–70.
9. Erkut B, Onk OA. Effect of N-acetylcysteine and allopurinol combination to protect spinal cord ischemia/reperfusion injury induced by aortic cross-clamping in rat model. J Cardiothorac Surg. 2015;10(1):1.
10. Charles AL, Guilbert AS, Bouitbir J, Marco GD, Enache I, Zoll J, et al. Effect of postconditioning on mitochondrial dysfunction in experimental aortic cross-clamping. Br J Surg. 2011;98(4):511–6.
11. Pottecher J, Guillot M, Belaidi E, Charles AL, Lejay A, Gharib A, et al. Cyclosporine A normalizes mitochondrial coupling, reactive oxygen species production, and inflammation and partially restores skeletal muscle maximal oxidative capacity in experimental aortic cross-clamping. J Vasc Surg. 2013;57(4):1100–8.
12. Guillot M, Charles AL, Chamaraux-Tran TN, Bouitbir J, Meyer A, Zoll J, et al. Oxidative stress precedes skeletal muscle mitochondrial dysfunction during experimental aortic cross-clamping but is not associated with early lung, heart, brain, liver, or kidney mitochondrial impairment. J Vasc Surg. 2014;60(4):1043–51.
13. Kalder J, Keschenau P, Hanssen SJ, Greiner A, Windsant IC, Kennes LN, et al. The impact of selective visceral perfusion on intestinal macrohemodynamics and microhemodynamics in a porcine model of thoracic aortic cross-clamping. J Vasc Surg. 2012;56(1):149–58.
14. Armentano RL, Cymberknop LJ, Legnani W, Pessana FM, Craiem D, Graf S, Barra JG. Arterial pressure fractality is highly dependent on wave reflection. In: 2013 35th Annual International Conference of the IEEE Engineering in Medicine and Biology Society (EMBC), 2013; Jul 3: 1960–1963.
15. Swillens A, Segers P. Assessment of arterial pressure wave reflection: methodological considerations. Artery Res. 2008;2(4):122–31.
16. Fantini F, Mattocks A, Bulpitti CJ, Banya W, Rajkumari C. Is augmentation index a good measure of vascular stiffness in the elderly? Age Ageing. 2007;36:43–8.
17. Liao J, Farmer J. Arterial stiffness as a risk factor for coronary artery disease. Curr Atheroscler Rep. 2014;16:387.
18. O'Rourke MF, Staessen JA, Vlachopoulos C, Duprez D, Plante GE. Clinical applications of arterial stiffness: definitions and reference values. Am J Hypertens. 2002;15:426–44.
19. Westerhof N, Sipkema P, Vanden Bos GC, Elzinga G. Forward and backward waves in the arterial system. Cardiovasc Res. 1972;6:648.
20. Westerhof BE et al. Quantification of wave reflection in the human aorta from pressure alone: a proof of principle. Hypertension. 2006;48:595–601.
21. Politi MT, Ghigo A, Fernández JM, Khelifa I, Gaudric J, Fullana JM, et al. The dicrotic notch analyzed by a numerical model. Comput Biol Med. 2016;72:54–64.
22. Borlotti A, Li Y, Parker KH, Khir AW. Experimental evaluation of local wave speed in the presence of reflected waves. J Biomech. 2004;47(1):87–95.

23. Khir AW, Parker KH. Measurements of wave speed and reflected waves in elastic tubes and bifurcations. J Biomech. 2002;35(6): 775–83.

24. Beckmann M, Jacomella V, Kohler M, Lachat M, Salem A, Amann-Vesti B, et al. Risk stratification of patients with peripheral arterial disease and abdominal aortic aneurysm using aortic augmentation index. PLoS One. 2015;10(10):e0139887.

25. Murgo JP, Altobelli SA, Dorethy JF, Logsdon JR, McGranathan GM: Normal ventricular ejection dynamics in man during rest and exercise. In: Physiologic Principles of Heart Sounds and Murmurs, Leon DF, Shaver JA. Dallas, American Heart Association, 1975, p 92.

26. Murgo JP, Westerhof N, Giolma JP, Altobelli SA. Aortic input impedance in normal man: relationship to pressure wave forms. Circulation. 1980;62(1):105–16.

27. Mandelbrot BB. Fractals: form, chance, and dimensions. San Francisco: Freeman; 1977. **365 pp**.

28. Zamir M. Arterial branching within the confines of fractal L-system formalism. J Gen Physiol. 2001;118(3):267–76.

29. Bassingthwaighte JB. Fractal vascular growth patterns. Acta Stereologica. 1992;11 Suppl 1:305.

30. Cymberknop LJ, Armentano RL, Pessana F, Alfonso MR, Legnani WE. Mapping the fractal dimension of arterial pressure. IUPESM 2015. World Congress on Medical Physics & Biomedical Engineering 2015; 7–12.

31. Cymberknop LJ, Legnani W, Pessana FM, Crottogini A, Armentano RL.Coronary arterial stiffness is related with a loss of fractal complexity in the aortic pressure. 2012 Annual International Conference of the IEEE Engineering in Medicine and Biology Society 2012; 4200–03.

32. Sharma V. Deterministic chaos and fractal complexity in the dynamics of cardiovascular behavior: perspectives on a new frontier. Open Cardiovasc Med J. 2009;3:110–23.

33. Cymberknop LJ, Legnani W, Pessana FM, Bia D, Zócalo Y, Armentano RL. Stiffness indices and fractal dimension relationship in arterial pressure and diameter time series in-vitro. J Phys Conf Ser. 2011;332:12–24.

34. World Medical Association. World Medical Association Declaration of Helsinki. Ethical principles for medical research involving human subjects. Bull World Health Organ. 2001;79(4):373.

35. Liu C, Zheng D, Murray A, Liu C. Modeling carotid and radial artery pulse pressure waveforms by curve fitting with Gaussian functions. Biomed Signal Process Control. 2013;8(5):449–54.

36. Liu C, Zhao L, Liu C. Effects of blood pressure and sex on the change of wave reflection: evidence from gaussian fitting method for radial artery pressure waveform. PLoS One. 2014;9(11): e112895.

37. Takazawa K, Tanaka N, Takeda K, Kurosu F, Ibukiyama C. Underestimation of vasodilator effects of nitroglycerin by upper limb blood pressure. Hypertension. 1995;26(3):520–3.

38. Gallagher D, Adji A, O'Rourke MF. Validation of the transfer function technique for generating central from peripheral upper limb pressure waveform. Am J Hypertens. 2004;17(11):1059–67.

39. Higuchi T. Approach to an irregular time series on the basis of the fractal theory. Phys D. 1988;31:277–83.

40. Laurent S, Cockcroft J, Van Bortel L, Boutouyrie P, Giannattasio C, Hayoz D, et al. Expert consensus document on arterial stiffness: methodological issues and clinical applications. Eur Heart J. 2006;27(21):2588–605.

41. Nichols WW, Edwards DG. Arterial elastance and wave reflection augmentation of systolic blood pressure: deleterious effects and implications for therapy. J Cardiovasc Pharmacol Ther. 2001;6(1):5–21.

42. Mills CJ, Gabe IT, Gault JH, Mason DT, Ross Jr J, Braunwald E, et al. Pressure flow relationships and vascular impedance in man. Cardiovasc Res. 1970;4:405.

43. Latham RD, Westerhof N, Sipkema P, Rubal BJ, Reuderink P, Murgo JP. Regional wave travel and reflections along the human aorta: a study with six simultaneous micromanometric pressures. Circulation. 1985;72(6):1257–69.

44. Crystal H, Holman S, Lui YW, Baird A, Yu H, Klein R, et al. Association of the fractal dimension of retinal arteries and veins with quantitative brain MRI measures in HIV-infected and uninfected women (P4. 067). Neurology. 2016;86(16 Supplement):P4–067.

45. Gryglewska B, Nęcki M, Żelawski M, Cwynar M, Baron T, Mrozek M, et al. Fractal dimensions of skin microcirculation flow in subjects with familial predisposition or newly diagnosed hypertension. Cardiol J. 2011;18(1):26–32.

46. Takahashi T. Microcirculation in fractal branching networks. Springer Japan 2014.